THE JOURNAL OF BIOLOGICAL CHEMISTRY VOL. 289, NO. 2, pp. 765–777, January 10, 2014

Homo-oligomerization of the Activating Natural Killer Cell Receptor NKp30 Ectodomain Increases Its Binding Affinity for Cellular Ligands*

Received for publication, September 4, 2013, and in revised form, November 12, 2013 Published, JBC Papers in Press, November 25, 2013, DOI 10.1074/jbc.M113.514786

Julia Herrmann[‡], **Hannah Berberich**[‡1], **Jessica Hartmann**[‡2], **Steffen Beyer**[‡], **Karen Davies**[§], **and Joachim Koch**[‡3]

From the [‡]*NK Cell Biology, Georg-Speyer-Haus, Institute for Tumor Biology and Experimental Therapy, D-60596 Frankfurt am Main, Germany and* [§]*Department of Structural Biology, Max Planck Institute of Biophysics, D-60438 Frankfurt am Main, Germany*

Background: Immunosurveillance of cancer and infections by natural killer (NK) cells depends on the receptor NKp30.
Results: NKp30 forms homo-oligomers for high affinity binding to B7-H6 on malignantly transformed cells.
Conclusion: NKp30-dependent signaling of NK cells is increased by homo-oligomerization via its ectodomain.
Significance: This is the first study on NKp30 clustering to strengthen the NK cell-target cell interaction.

The natural cytotoxicity receptors, comprised of three type I membrane proteins NKp30, NKp44, and NKp46, are a unique set of activating proteins expressed mainly on the surface of natural killer (NK) cells. Among these, NKp30 is a major receptor targeting virus-infected cells, malignantly transformed cells, and immature dendritic cells. To date, only few cellular ligands of NKp30 have been discovered, and the molecular details of ligand recognition by NKp30 are poorly understood. Within the current study, we found that the ectodomain of NKp30 forms functional homo-oligomers that mediate high affinity binding to its corresponding cellular ligand B7-H6. Notably, this homo-oligomerization is strongly promoted by the stalk domain of NKp30. Based on these data, we suggest that homo-oligomerization of NKp30 in the plasma membrane of NK cells, which might be favored by IL-2-dependent up-regulation of NKp30 expression, provides a way to improve recognition and lysis of target cells by NK cells.

Natural killer (NK)[4] cells are large granular lymphocytes of the innate immune system that spontaneously kill foreign, tumor, and virus-infected cells without prior sensitization via the polarized release of cytotoxic granules that are loaded with perforin and granzymes (1–6). Additionally, NK cells act as immune regulators by secretion of chemokines and cytokines and by direct interaction with other immune cells such as dendritic cells (7, 8). NK cells are regulated by the integration of signals triggered by ligands binding to different activating and inhibitory germ line-encoded surface receptors (1, 2, 4, 9–16). The balance of activating and inhibitory receptor stimulation determines the activation state of NK cells. The inhibitory receptors on human NK cells comprise receptors that mostly recognize MHC class I molecules on the surface of target cells; however, some non-MHC class I ligands are also recognized (15). Among the major human activating NK cell receptors, the natural cytotoxicity receptors (NCRs) NKp30 (NCR3, CD337), NKp44 (NCR2, CD336), and NKp46 (NCR1, CD335) recognize stress-induced or *de novo* expressed ligands on target cells (17–21). The NCR family members are type I membrane proteins of the immunoglobulin (Ig) superfamily that comprise an extracellular ligand binding domain (LBD) with a flexible membrane proximal stalk region, a transmembrane domain, and a short cytosolic tail. Because of the lack of intracellular activating signaling motifs, the NCRs associate with immunoreceptor tyrosine-based activating motif-bearing adaptor molecules via oppositely charged amino acid residues within the plasma membrane (4, 17–21). The NCRs play a pivotal role for the elimination of parasites, malignantly transformed and virus-infected cells, and even some healthy cells (15). Notably, cytokines such as IL-2, which promote NK cell activation, lead to a drastic increase of plasma membrane expression of the NCRs and thus cellular cytotoxicity (22–27).

Previously, viral hemagglutinins and proteins from bacterial or parasitical origin were identified as ligands of the NCRs (4). However, to date, only few cellular ligands of the NCRs are known. In immunosurveillance of malignantly transformed cells, NKp30 recognizes the tumor antigens B7-H6 (11, 28) and BCL-2-associated athanogene 6 (BAG-6, also known as BAT3) (29–33) triggering NK cell cytotoxicity.

The stalk domain of NKp30 increases the binding affinity of the receptor for its cellular ligands BAG-6 and B7-H6, thus, representing an important module for ligand recognition (34). However, the precise mode of action of the stalk domain has not been elucidated yet. Additionally, recent data suggest that the glycosylation status of NKp30 at its three extracellular *N*-linked glycosylation targeting sites provides a novel mechanism that facilitates the modulation of the ligand binding properties of NKp30 and related NK cell cytotoxicity (34).

* This work was supported by institutional funds of the Georg-Speyer-Haus and by grants from the Schleicher Stiftung and the LOEWE Center for Cell and Gene Therapy Frankfurt funded by Hessisches Ministerium für Wissenschaft und Kunst (HMWK) reference number III L 4-518/17.004 (2010).

[1] Present address: Institute of Molecular Biology and Tumor Research, University of Marburg, D-35032 Marburg, Germany.
[2] Present address: Molecular Biotechnology and Gene Therapy, Paul-Ehrlich-Institut, D-63225 Langen, Germany.
[3] To whom correspondence should be addressed: Georg-Speyer-Haus, Institute for Biomedical Research, Paul-Ehrlich-Strasse 42-44, D-60596 Frankfurt am Main, Germany. Tel.: 49-69-63395-322; Fax: 49-69-63395-297; E-mail: joachim.koch@gsh.uni-frankfurt.de.

[4] The abbreviations used are: NK, natural killer; NCR, natural cytotoxicity receptor; LBD, ligand binding domain; CLSM, confocal laser scanning microscopy; B_{max}, maximum number of receptor binding sites.

Among the NCRs, NKp30 is the only receptor whose structure has been solved in an unbound (35) and in a ligand-bound (36) state. Interestingly, although both structures show NKp30 as a monomer, Sun and co-workers (35) observed a crystallographic dimer of NKp30 arguing for a potential intrinsic capability of NKp30 to oligomerize. Similarly, Bordo and co-workers (37) discussed a saddle-shaped dimer within the crystal structure of NKp44 that is exclusively expressed on activated NK cells. Along these lines, Porgador and co-workers (38) show that the membrane proximal domain of NKp46 (NKp46D2) mediates ligand-induced dimerization of NKp46 in the membrane and contributes to NKp46-mediated lysis by NK cells. Further evidence to support the idea of NCR self-assembly is scarce. However, NK cell killing requires the formation of a complex immunological synapse between the target cell and the NK cell that is highly organized in time and space (39–41), which argues for concerted lateral interactions of receptors at the plasma membrane of the NK cell engaged with a target cell. Moreover, many laboratories have shown that cell surface detection of NKp30 on NK cell lines or primary NK cells with NKp30-specific monoclonal antibodies gives rise to dotted rather than a homogeneous plasma membrane staining suggesting preformed clusters of NKp30. Interestingly, Bezouška and co-workers (42) have shown that a fraction of NKp30 expressed in *Escherichia coli* forms oligomers as detected by size exclusion chromatography. However, the authors have not analyzed this fraction of NKp30 in more detail. Within the current study, we therefore investigated whether the NKp30 ectodomain has the intrinsic ability to form oligomers, which might impact ligand binding affinity and the efficiency of target cell killing by NK cells.

MATERIALS AND METHODS

Antibodies—Antibodies used for immunoprecipitation and immunoblot were anti-NKp30, clone P30–15 (kindly provided by C. Watzl, IfADo, Dortmund, Germany), anti-NKp30, polyclonal (AF1849, R&D Systems), and anti-goat-IgG (HRP conjugate; 705-036-147, Jackson ImmunoResearch). Antibodies for ELISA were anti-NKp30, clone 210845 (MAB1849, R&D Systems), anti-NKp30, polyclonal (AF1849, R&D Systems), anti-MICA, polyclonal (AF1300, R&D Systems), anti-goat-IgG (HRP conjugate; 705-036-147, Jackson ImmunoResearch), and anti-human-IgG-Fc (HRP conjugate, A0170, Sigma). For flow cytometry and confocal immunofluorescence microscopy anti-NKp30, clone 210845 (MAB1849, R&D Systems), anti-mouse-IgG (Alexa647 conjugate; A21236, Life Technologies), anti-human-IgG-Fc (DyLight649 conjugate; 109–495-008, Jackson ImmunoResearch), anti-NKp30, purified from rabbit serum after immunization with the antigenic peptide NH2-CPGKEV-RNGTPEFRGR-COOH (BioScience/pepScience, Göttingen, Germany), and anti-rabbit-IgG (allophycocyanin conjugate; A10931, Life Technologies) were used. Anti-mouse-CD4, clone GK1.5 (allophycocyanin conjugate; 17-0041-81, eBioScience) was used for the signaling reporter assay.

Cell Lines—*Spodoptera frugiperda* insect cells (*Sf*9, 11496-015, Invitrogen) were maintained at 27 °C and 90 rpm in Insect-XPRESS medium (Lonza) supplemented with 0.2% (v/v) Pluronic F-68 (Sigma). *Trichoplusia ni* insect cells (High Five, B855–02, Invitrogen) were cultivated at 27 °C and 90 rpm in Express Five SFM (Invitrogen) supplemented with 18 mM L-glutamine. Human embryonic kidney cells (293T/17, CRL-11268) were purchased from American Type Culture Collection (ATCC) and maintained under standard conditions. Murine pro B cells (Ba/F3 cells) were purchased from Deutsche Sammlung von Mikroorganismen und Zellkulturen. Ba/F3 cells transduced with B7-H6 (Ba/F3-B7-H6) or the empty vector (Ba/F3-GFP) were kindly provided by C. Watzl (IfADo) and cultivated as described (43). Murine A5 T cell hybridoma cells ($CD4^+$) transduced with retrovirus encoding full-length NKp30 fused to a C-terminal decahistidine tag (A5-30FL-His) or a mock control (A5-GFP) were kindly provided by A. Diefenbach (University of Freiburg, Germany) (34, 44).

Isolation and Cultivation of NK Cells—The natural killer cell line NK-92MI (ATCC CRL-2408) was maintained in RPMI medium supplemented with 10% (v/v) FCS (PAA), 10% (v/v) horse serum (PAA), 100 units/ml penicillin, 100 μg/ml streptomycin, 1 mM sodium pyruvate, and 4 mM L-glutamine.

Primary human natural killer cells were isolated from buffy coats (kindly provided by H. Bönig, German Red Cross Blood Service, Institute for Transfusion Medicine and Immunohematology, Medical School, Goethe-University, Frankfurt, Germany) by a Ficoll gradient (Biozol) and magnetic-activated cell sorting for untouched NK cells (130-092-657, Miltenyi Biotech). Cells were cultivated and expanded for 7 days in X-Vivo 10 (Lonza), 5% (v/v) human serum (PAA), 1000 units/ml IL-2 (PromoKine), and activation beads (130-094-483, Miltenyi Biotech).

Protein Expression and Purification—The full-length NKp30 receptor (NKp30-His) as well as the soluble NKp30 ectodomain proteins without the stalk domain (30LBD-His) and including the stalk domain (30Stalk-His) were expressed in insect cells using the baculovirus expression system. For the expression of NKp30-His, the cDNA sequence of human NKp30 (NCB accession number NM_147130.2; amino acids 1–201) with an additional sequence coding for a C-terminal decahistidine tag was cloned into the MultiBac acceptor plasmid pFL (kindly provided by I. Berger, EMBL, Grenoble, France) (45) via the XbaI and the StuI restriction sites. To express soluble NKp30 ectodomain proteins, the gp67 secretion sequence and an additional ADLGS sequence (46) were added N-terminal to the sequence coding for the ectodomain of human NKp30 (NCB accession number NM_147130.2; 30Stalk-His, amino acids 19–143; 30LBD-His, amino acids 19–128). The C terminus of the NKp30 ectodomain variants was fused to a tobacco etch virus (TEV) cleavage site (GS-ENLYFQ-GGS; the glycine-serine linker-flanked TEV cleavage site is underlined) followed by a decahistidine tag. Both constructs encoding 30Stalk-His and 30LBD-His proteins were generated by *de novo* gene synthesis (GenScript) and cloned into the pFastBac1 vector (Invitrogen) using the restriction sites XhoI and HindIII. Recombinant baculoviruses were generated as described elsewhere (45). *Sf*9 insect cells were transfected with recombinant bacmids in 6-well plates according to the manufacturer (5 μg bacmid-DNA/10^6 cells/6-well) using the *Trans*IT-LT1 transfection reagent (MIRUS). 60 h after transfection, the initial virus-containing supernatant (V_0) was collected and used for infection of

a *Sf*9 suspension culture (7×10^5 cells/ml, 25 ml). Suspension cultures of infected cells were split every 24 h until cell proliferation arrest occurred. 48 h after proliferation arrest, the amplified virus (V_1) was collected and used for protein production by infecting High Five insect cells (1 ml of V_1/100 ml of suspension culture, 7×10^5 cells/ml). Roughly 72 h after infection, High Five insect cells were harvested to investigate NKp30-His expression, or the cell culture supernatant of the infected High Five insect cells was collected to purify the secreted NKp30 ectodomain proteins 30Stalk-His or 30LBD-His. The NKp30 ectodomain protein-containing supernatants were ultracentrifuged (100,000 × *g*, 2 h, 4 °C) to remove baculovirus particles, dialyzed (50 mM Tris, 500 mM NaCl, 10 mM imidazole, pH 8, 4 °C), and affinity-purified using nickel-nitrilotriacetic acid-agarose beads (Macherey-Nagel). Buffer exchange (50 mM Tris, 150 mM NaCl, pH 8, 4 °C) and concentration of the soluble NKp30 ectodomain proteins were performed using Amicon Ultra filters (molecular weight cutoff, 3 kDa; Merck Millipore). The production of the B7-H6::hIgG1-Fc (B7-H6-Ig) protein (NCB accession number NM_001202439.1; amino acids 25–227, expression plasmid kindly provided by C. Watzl, IfADo) was described elsewhere (34). The extracellular domain of human MICA*04 (UniProt Q29983; amino acids 24–299, expression plasmid kindly provided by A. Steinle, Institute for Molecular Medicine, Goethe University, Frankfurt am Main, Germany), fused to a C-terminal hexahistidine tag (MICA*04-His), was refolded from *E. coli* inclusion bodies and affinity-purified (47).

Immunoprecipitation and Immunoblot—To analyze the expression of NKp30-His proteins by infected High Five insect cells, each 10^7-infected and non-infected (control) High Five cells were resuspended in lysis buffer (20 mM Tris, 150 mM NaCl, 10% (v/v) glycerol, 0.5% (v/v) Triton X-100, 2 mM EDTA, 10 mM NaF, 1 mM phenylmethylsulfonyl fluoride, pH 7.4), incubated on ice for 20 min, and centrifuged for 30 min (20,000 × *g*, 4 °C). For immunoprecipitation of NKp30, anti-NKp30 antibodies (clone P30-15) were added to the cell lysates and incubated for 4 h at 4 °C followed by addition of Protein A Dynabeads (Invitrogen) and overnight incubation at 4 °C. The protein-antibody complexes were eluted from the beads according to the manufacturer. Immunoblot analyses of NKp30-His and soluble NKp30 ectodomain proteins were performed using a polyclonal anti-NKp30 antibody.

Deglycosylation Assays—Treatment of 30Stalk-His and 30LBD-His proteins with glycosidases either removing only *N*-linked (peptide-*N*-glycosidase F, New England Biolabs) or *N*- and *O*-linked oligosaccharides (protein deglycosylation mix, New England Biolabs) was performed according to the manufacturer. Molecular mass reduction of the deglycosylated proteins was investigated by reducing SDS-PAGE and immunoblot. To inhibit *N*-linked glycosylation during protein expression, 0.5 μg/ml tunicamycin (Sigma) was added once to the insect cell culture 1 h post infection followed by the standard protein expression procedure.

Size Exclusion Chromatography—The oligomerization state of 30Stalk-His and 30LBD-His proteins was analyzed by size exclusion chromatography at different buffer conditions (50 mM Tris, 150 mM NaCl, pH 8, 4 °C, 50 mM Tris, 500 mM NaCl, pH 8 at 4 °C or PBS (PAA) at 4 °C) with a flow rate of 0.5 ml/min using a Superdex 200 10/300 GL column (GE Healthcare). 500 μl elution fractions were collected. For electron microscopy of the 30Stalk-His and 30LBD-His oligomers, size exclusion chromatography was performed in 50 mM Tris, 150 mM NaCl, pH 8, 4 °C with a flow rate of 0.3 ml/min using a Superose 6 10/300 GL column (GE Healthcare). 100 μl elution fractions were collected.

Negative-stain Electron Microscopy (EM)—To analyze the geometry and three-dimensional arrangement of the NKp30 ectodomain oligomers, the elution fractions of the size exclusion chromatography (Superose 6 10/300 GL column) with the highest protein amount were chosen. The concentration of the oligomers was adjusted to 0.1 mg/ml. Samples were diluted 1:4 (30Stalk-His) or 1:25 (30LBD-His) with buffer (50 mM Tris, 150 mM NaCl, pH 8, 4 °C). 3 μl of sample were applied to glow-discharged EM grids (400 mesh) containing a continuous carbon support film. After 1 min, the samples were washed dropwise with 20 μl of 1% (w/v) uranyl acetate and then incubated with 3 μl of stain for a further minute. Excess stain was removed with filter paper (#4, Whatman). Electron microscopy was performed using a Tecnai Spirit electron microscope (FEI, Eindhoven, The Netherlands) operating at 120 kV. Images were acquired at a nominal magnification of 34,000× on a 4,096 × 4,096 pixel CCD (Ultrascan 4000, Gatan), which corresponds to a specimen pixel size of 0.36 nm.

Enzyme-linked Immunosorbent Assay (ELISA)—96-Well plates (Greiner) were coated with recombinant B7-H6-Ig protein (1 μg/well), blocked with 7.5% (w/v) BSA in PBS, and probed with graded amounts (0–400 nM) of the NKp30 ectodomain proteins or MICA*04-His as control protein. To block the interaction between B7-H6-Ig and the recombinant NKp30 ectodomain proteins, the dilution series was preincubated with anti-NKp30 antibody (67 nM, clone 210845) for 1 h. The amount of bound NKp30 ectodomain proteins was quantified after immunodetection (anti-NKp30, polyclonal) and visualization with 3,3′,5,5′-tetramethylbenzidine substrate in a microtiter plate reader ($\lambda = 450$ nm). K_D and B_{max} values were determined after fitting the curves to a 1:1 Langmuir binding model using Prism 5 software (GraphPad). To determine the K_D and B_{max} values of the individual oligomers, dimers and monomers of 30Stalk-His, the respective proteins, or 1 μg/well of 30Stalk-His mixture were coated and probed with graded amounts (0–400 nM) of the recombinant B7-H6-Ig fusion protein. Immunodetection was performed with an anti-human-IgG-Fc antibody.

Flow Cytometry and Confocal Immunofluorescence Studies—Cells were washed and blocked with 5% (w/v) BSA in PBS supplemented with 2% (v/v) FCS. NKp30-His proteins on infected High Five insect cells were immunostained with an anti-NKp30 antibody (clone 210845). Furthermore, High Five insect cells infected with baculovirus particles encoding NKp30-His protein were incubated with B7-H6-Ig fusion protein (50 μg/ml), and immunostaining was performed using a DyLight649-coupled anti-human-IgG-Fc antibody. Ba/F3 cells and primary NK cells were decorated with NKp30 ectodomain proteins (50 μg/ml) or NKp30 ectodomain proteins preincubated with a blocking antibody (75–250 μg/ml, anti-NKp30, clone 210845).

After immunostaining (anti-NKp30, purified from rabbit serum), cells were fixed with 1% (v/v) formaldehyde. A minimum of 50,000 cells was analyzed with a FACSCanto II flow cytometer and BD DIVA 6.0 software (BD Bioscience). For confocal immunofluorescence microscopy, cells were additionally stained with DAPI (10 μg/ml, AppliChem) before microscopy with a TCS-SP5 confocal laser scanning microscope (CLSM, Leica; LAS-AF lite 2.0 software).

Quantification of Cell Decoration—Images of single B7-H6-transduced Ba/F3 cells decorated with 30Stalk-His ($n = 42$) and 30LBD-His ($n = 56$) proteins were quantitatively analyzed using the cell image analysis software CellProfiler (48). NKp30 ectodomain protein clusters (diameter of 4–40 pixels) were identified on grayscale images of the APC channel by pixel intensity (thresholding method: kapur global; correction factor: 2). The cluster area was determined as actual number of pixels in the region. Statistical significance was determined by the Mann-Whitney test using the Prism 5 software (Graph Pad): not significant, >0.05; *, $p = 0.01–0.05$; **, $p = 0.001–0.01$; ***, $p < 0.001$.

Signaling Reporter Assay—A5-30FL-His effector cells were mixed with 50,000 Ba/F3-B7-H6 target cells at effector:target ratios of 2:1, 1:1, and 0.5:1. For signal inhibition, Ba/F3-B7-H6 target cells were preincubated with the NKp30-Ig fusion protein or the NKp30 ectodomain proteins for 1 h at 37 °C followed by co-incubation with A5-30FL-His effector cells for 16 h at 37 °C. Cells were stained with an anti-mouse-CD4 antibody to discriminate effector from target cells. GFP expression of the $CD4^+$ A5-30FL-His effector cells was determined with a FACSCanto II flow cytometer and BD DIVA 6.0 software (BD Bioscience).

RESULTS

Expression of Functional NKp30 in Insect Cells—Insect cells have a proven record for the expression of correctly folded and post-translationally modified human proteins. Therefore, we investigated whether insect cells are a suitable expression host for the production of human NKp30. Ovarian cells of the cabbage looper (*T. ni*, High Five cells) were infected with baculovirus particles containing the cDNA sequence of the human NKp30 full-length receptor with an additional sequence coding for a C-terminal decahistidine tag (Fig. 1*A*). 72 h after infection, NKp30-His was immunoprecipitated from cell lysates with a monoclonal NKp30-specific antibody and analyzed by immunoblot using a polyclonal NKp30-specific antibody. NKp30-His (predicted molecular mass from primary sequence, 23 kDa) was detected as a protein band with an apparent molecular mass of roughly 30 kDa, indicating post-translational modification of NKp30-His (Fig. 1*B*). To investigate whether NKp30-His is targeted to the plasma membrane of insect cells, we performed CLSM and flow cytometry analyses with a monoclonal NKp30-specific antibody. NKp30-His was exclusively found on the plasma membrane of infected cells (Fig. 1, *C* and *D*). Moreover, these data suggest that the overall folding of NKp30-His is correct as it has passed the endoplasmic reticulum quality control. To prove that NKp30-His adopts a ligand binding-receptive conformation, we performed CLSM and flow cytometry analyses with recombinant B7-H6-Ig fusion protein (Fig. 1, *E* and *F*). Strikingly, the recombinant ligand B7-H6-Ig was detected only at the plasma membrane of High Five insect cells infected with recombinant baculovirus encoding NKp30-His, demonstrating that NKp30-His expressed in insect cells is functionally equivalent to that derived from human expression hosts.

Expression of Soluble Variants of the NKp30 Ectodomain in Insect Cells—We have previously shown that the membrane proximal stalk domain and glycosylation status of NKp30 impact ligand binding (34). In this study, the ectodomain of NKp30 was fused to a human IgG1-Fc part generating a bivalent and potentially dimeric receptor molecule. To date, the oligomeric state of NKp30 is unknown. Because oligomerization of NKp30 could be a mechanism to improve ligand binding affinity and corresponding cytotoxicity of the NK cell, we analyzed soluble variants of the ectodomain of NKp30 produced in insect cells. In analogy to the NKp30::IgG1-Fc fusion proteins (34), we generated a construct comprising the globular Ig domain (30LBD-His, amino acids 19–128; Fig. 2*A*) and a construct comprising the entire ectodomain of NKp30 including its stalk domain (30Stalk-His, amino acids 19–143; Fig. 2*B*). Both constructs contain an N-terminal gp67 secretion sequence and a C-terminal decahistidine tag for affinity purification. Notably, both constructs contain the three previously identified acceptor sites for *N*-linked glycosylation (Asn-42, -68, and -121) (34). After infection of High Five insect cells with baculovirus particles encoding 30Stalk-His or 30LBD-His, both proteins were secreted into the culture medium and purified to homogeneity by immobilized metal ion affinity chromatography as demonstrated by non-reducing SDS-PAGE and corresponding immunoblot analyses with a polyclonal anti-NKp30 antibody (Fig. 2, *C* and *D*). The ectodomain of NKp30 contains two cysteines (Cys-39 and -108) that form an intramolecular disulfide bond (35, 36). To exclude the formation of artificial intermolecular disulfide bonds that might occur due to incomplete protein folding and exposure of reactive sulfhydryl groups, both NKp30 ectodomain proteins were investigated at reducing (+DTT) and non-reducing (−DTT) conditions. As shown by SDS-PAGE and corresponding immunoblot analyses, the 30Stalk-His or 30LBD-His proteins are identical in their apparent molecular mass at both conditions, indicating correct protein folding and the absence of artificial disulfide bonds (Fig. 2*E*). As expected from the results of full-length NKp30-His expression (see above), the apparent molecular mass of the 30-Stalk-His (20 *versus* 16.6 kDa) and the 30LBD-His protein (18 *versus* 15 kDa) differed from that predicted from primary sequence, suggesting post-translational modification. Glycosylation of the three acceptor sites for *N*-linked glycosylation within the ectodomain of NKp30 was analyzed by reducing SDS-PAGE and immunoblot analyses after enzymatic deglycosylation with peptide-*N*-glycosidase F (cleavage of *N*-linked glycans) or with an enzyme mix (cleavage of *N*- and *O*-linked glycans) (Fig. 2*F*). For both, the 30Stalk-His and the 30LBD-His protein, a distinct pattern of protein bands was observed due to incomplete deglycosylation corresponding to tri-, di-, and mono- and non-glycosylated proteins. Notably, modifica-

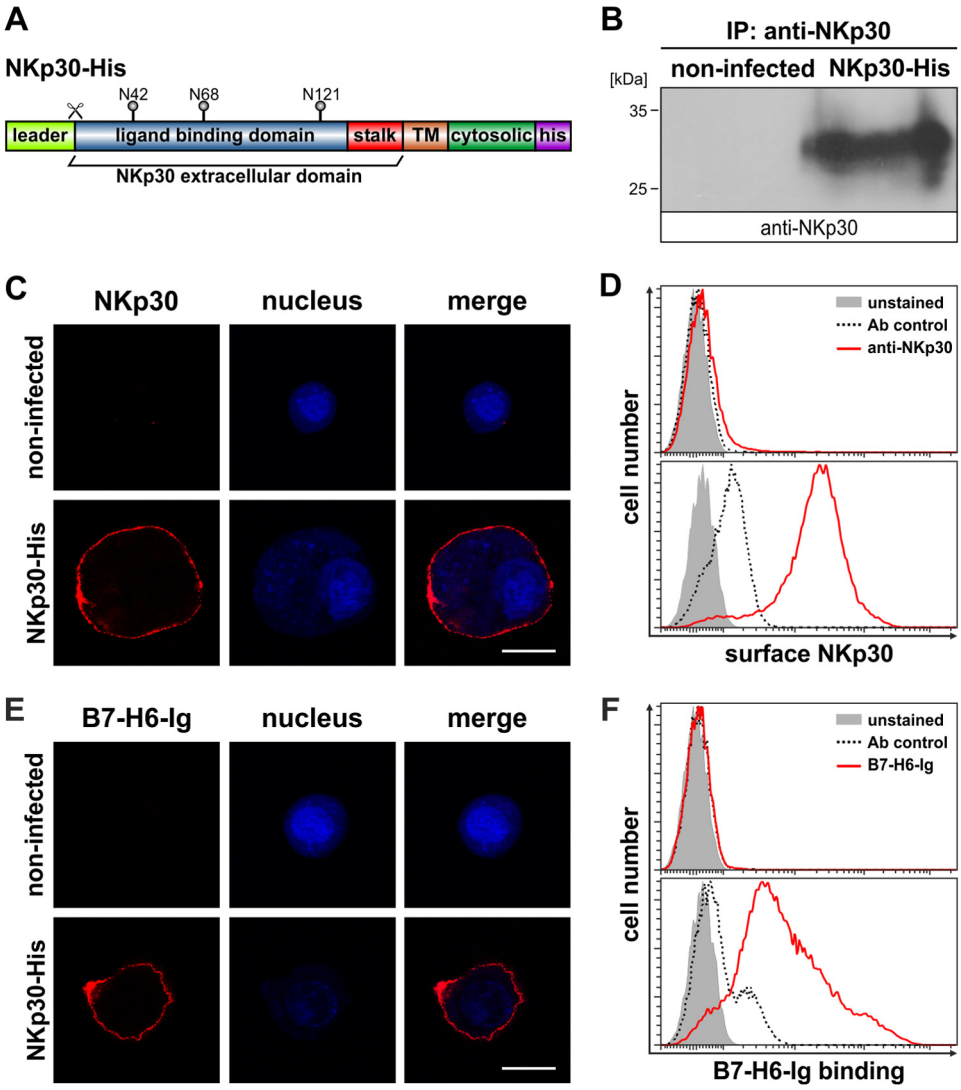

FIGURE 1. **Expression of functional NKp30 in insect cells.** *A*, domain organization of NKp30-His. *TM*, transmembrane domain; *his*, decahistidine tag; *N42*, *N68*, and *N121*, acceptor sites for *N*-linked glycosylation; *scissor*, cleavage site for leader sequence. *B*, immunoblot after immunoprecipitation (*IP*) of NKp30 (anti-NKp30) from lysates of NKp30-His infected or non-infected High Five insect cells. *C* and *D*, decoration of non-infected and NKp30-His infected High Five insect cells with an anti-NKp30 antibody to analyze NKp30 surface expression by CLSM (*red*, anti-NKp30; *blue*, DAPI; the *bar* corresponds to 20 μm) and flow cytometry (*solid gray*, unstained; *dashed line*, antibody control; *red line*, anti-NKp30). *E* and *F*, B7-H6-Ig fusion protein binding to non-infected and NKp30-His infected High Five insect cells was analyzed by CLSM (*red*, B7-H6-Ig fusion protein; *blue*, DAPI; the *bar* corresponds to 20 μm) and flow cytometry (*solid gray*, unstained; *dashed line*, antibody control; *red line*, B7-H6-Ig fusion protein).

tion of the assay conditions, such as increasing the amount of enzyme or extending the incubation time, did not influence the relative amount of differentially glycosylated forms of NKp30. Most likely this is due to insect cell-specific glycosylation of proteins with an α1–3 fucose residue at the innermost *N*-acetylglucosamine residue of the glycoprotein, which is resistant to peptide-*N*-glycosidase F cleavage. Therefore, we employed tunicamycin to inhibit the first step of *N*-linked glycosylation. Strikingly, tunicamycin treatment of the culture quantitatively blocked *N*-linked glycosylation of NKp30 (Fig. 2*G*). In conclusion, these studies show that the ectodomain of NKp30 produced in insect cells is *N*-linked-glycosylated at its three known acceptor sites (Asn-42, -68, and -121) in the absence of *O*-linked glycans and thus represents a molecular equivalent to the ectodomain of human NKp30 that can be employed for further studies.

The Ectodomain of NKp30 Binds with High Apparent Affinity to Its Cellular Ligand B7-H6—To examine the ligand binding properties of the soluble NKp30 ectodomain proteins and to study the contribution of the stalk domain of soluble NKp30 proteins to ligand binding, we performed cell decoration experiments, signaling reporter cell assays, and ELISA. For cell decoration experiments, NKp30 ligand-negative Ba/F3 cells stably transduced with the cellular NKp30 ligand B7-H6 and GFP (Ba/F3-B7-H6) or GFP only (Ba/F3-GFP) were incubated with 30Stalk-His and 30LBD-His proteins. Plasma membrane-attached NKp30 ectodomain proteins were visualized with an anti-NKp30 antibody by CLSM. Specific binding of the 30Stalk-His and 30LBD-His proteins to B7-H6 on the plasma membrane of Ba/F3-B7-H6 cells was detected (Fig. 3*A*). In accordance with our previous cell decoration studies with NKp30::IgG1-Fc fusion proteins (34), binding of

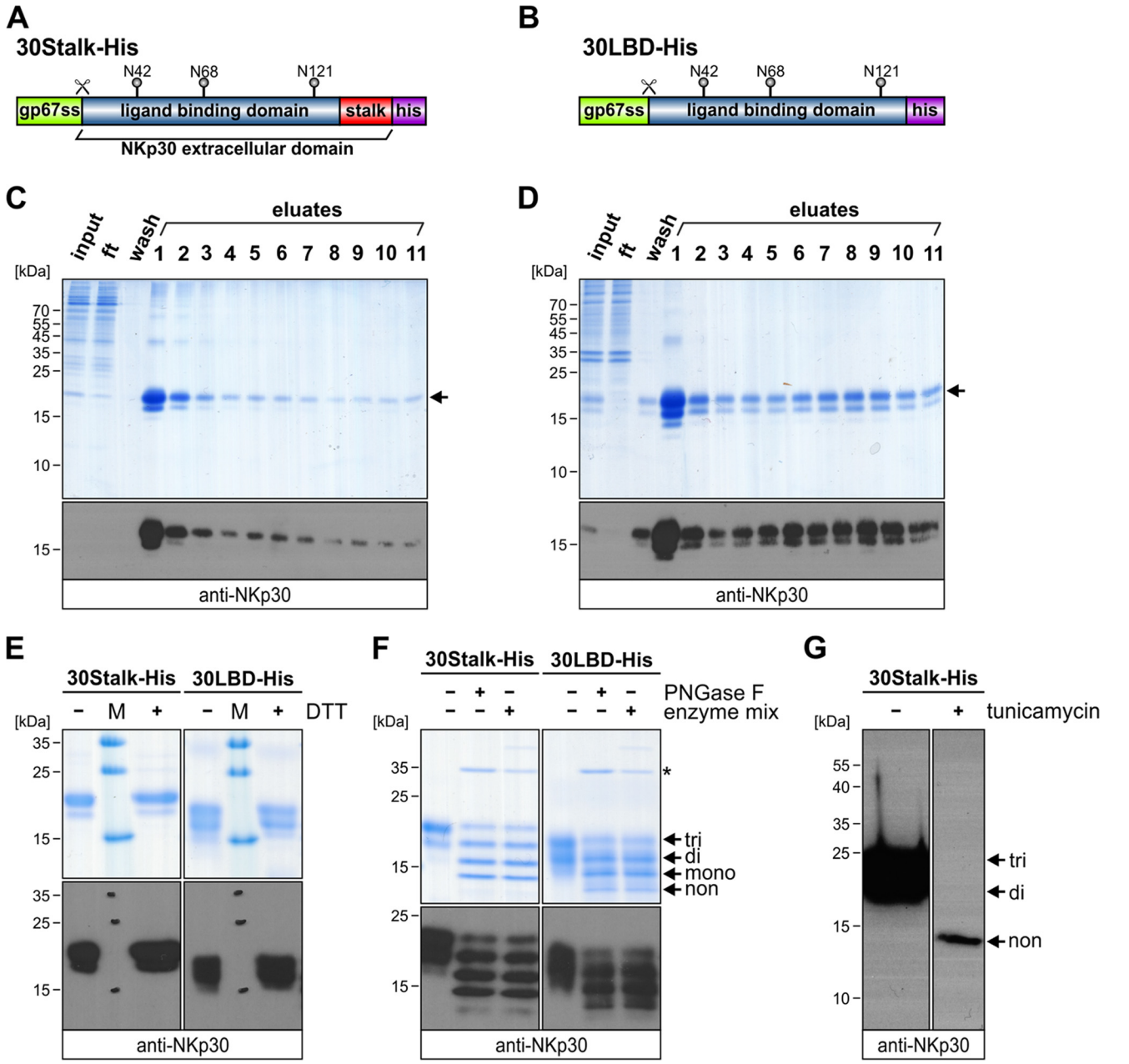

FIGURE 2. **Expression of soluble variants of the NKp30 ectodomain in insect cells.** Domain organization of 30Stalk-His (*A*) and 30LBD-His (*B*) is shown. *gp67ss*, glycoprotein 67 secretion sequence; *his*, decahistidine tag; *N42*, *N68*, and *N121*, acceptor sites for *N*-linked glycosylation; *scissor*, cleavage site for gp67 secretion sequence. *C* and *D*, non-reducing SDS-PAGE (Coomassie-stained) and immunoblot (anti-NKp30) of aliquots (input, flow-through, wash, and eluates) from purification of 30Stalk-His (*C*) and 30LBD-His proteins (*D*). *Arrow*, fully glycosylated NKp30 ectodomain protein. *ft*, flow-through. *E*, non-reducing (−DTT) and reducing (+DTT) SDS-PAGE (Coomassie-stained) and immunoblot (anti-NKp30) of purified 30Stalk-His and 30LBD-His proteins. *M*, protein marker. *F*, reducing SDS-PAGE (Coomassie-stained) and immunoblot (anti-NKp30) of untreated (*first lane*, 30Stalk-His; *fourth lane*, 30LBD-His), peptide-*N*-glycosidase F (*PNGase F*; *second lane*, 30Stalk-His; *fifth lane*, 30LBD-His) or enzyme mix-treated (*third lane*, 30Stalk-His; *sixth lane*, 30LBD-His) NKp30 ectodomain proteins. *Arrows*, tri-, di-, mono-, and non-glycosylated proteins. *Asterisk*, peptide-*N*-glycosidase F. *G*, immunoblot (anti-NKp30) of purified 30Stalk-His protein without (*first lane*) or with (*second lane*) tunicamycin treatment 1 h post infection prior to protein expression to inhibit *N*-linked glycoprotein synthesis. *Arrows*, tri-, di-, and non-glycosylated proteins.

soluble 30Stalk-His protein to plasma membrane B7-H6 was significantly stronger than that of 30LBD-His protein. This observation was nicely reflected by flow cytometry measurements performed with these cells. Also here, decoration of the Ba/F3-B7-H6 cells with 30Stalk-His protein led to much higher signal intensities when compared with 30LBD-His protein. For reference, no binding of the 30Stalk-His and 30LBD-His proteins was observed for the Ba/F3-GFP cells. Importantly, the receptor ligand interaction was highly specific as it could be quantitatively competed with an anti-NKp30 blocking antibody (Fig. 3*B*).

As demonstrated by representative NKp30 stainings of B7-H6-transduced Ba/F3 cells (Fig. 3*A*), a distinct dotted pattern was observed upon decoration with the 30Stalk-His and 30LBD-His proteins, suggesting formation of oligomeric receptor-ligand complexes. Quantitative analyses of a large number of cells revealed an equal average number of clusters per cell after binding of the NKp30 ectodomain proteins (Fig. 3*C*,

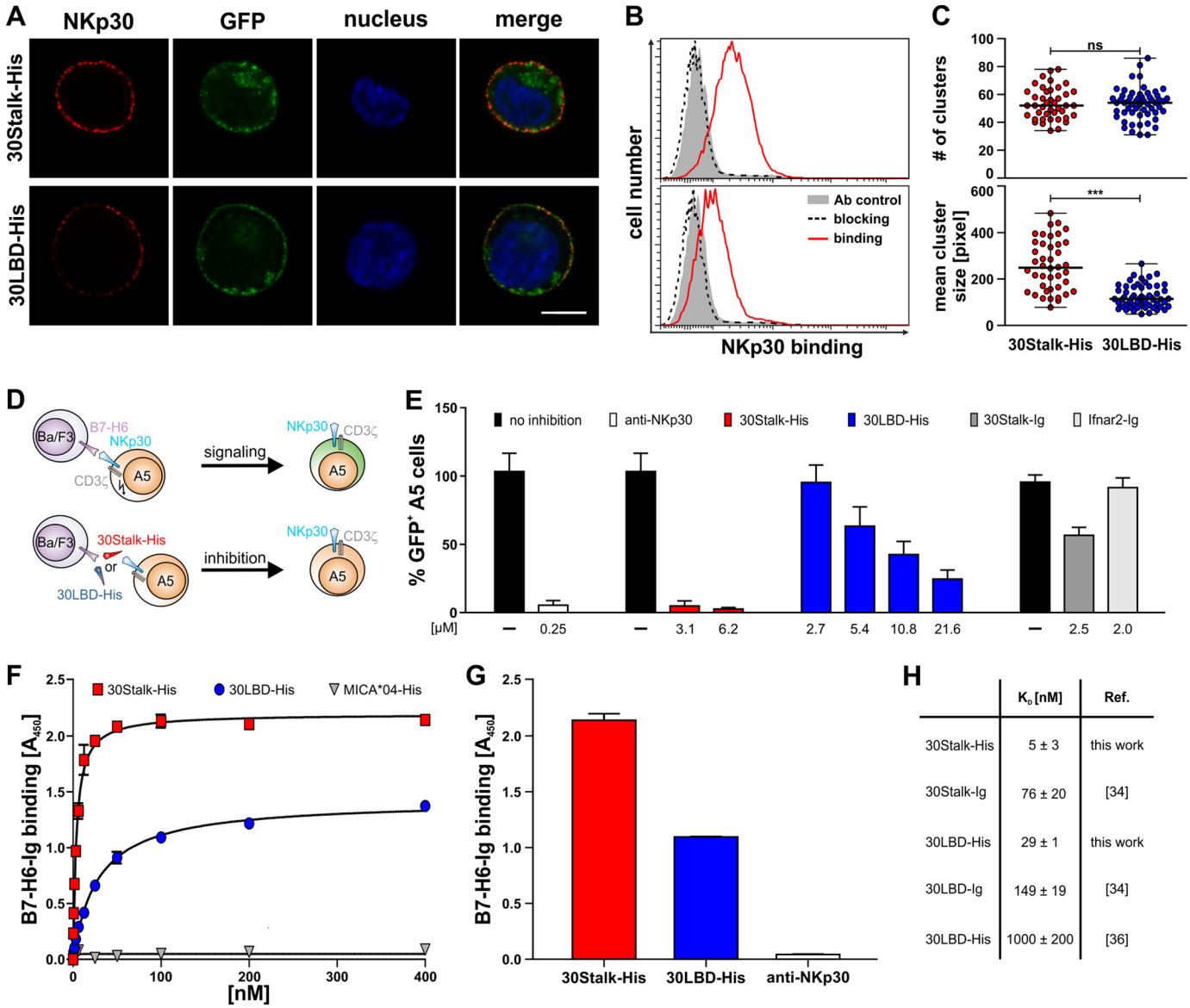

FIGURE 3. **Soluble NKp30 ectodomain proteins bind with high affinity to the cellular ligand B7-H6.** *A*, binding of 30Stalk-His or 30LBD-His proteins to B7-H6-transduced Ba/F3 cells was monitored by an anti-NKp30 antibody via CLSM (*red*, anti-NKp30; *green*, GFP; *blue*, DAPI; the *bar* corresponds to 5 μm). *B*, binding of 30Stalk-His and 30LBD-His proteins (*red line*) and specific blocking with an anti-NKp30 antibody (*dashed line*) were analyzed by flow cytometry (*solid gray*, antibody control). *C*, quantification of clusters observed on B7-H6 transduced Ba/F3 cells after decoration with 30Stalk-His and 30LBD-His proteins. Data points represent number of clusters (*upper panel*) and mean cluster size (*lower panel*) on a large number of individual cells decorated with 30Stalk-His (*red*) or 30LBD-His (*blue*) proteins. Mann-Whitney test: not significant (*ns*), $p = 0.9914$; ***, $p < 0.0001$. *D*, A5-30FL-His reporter cells were mixed with B7-H6 transduced Ba/F3 target cells. Upon NKp30-B7-H6 interaction, downstream signaling via CD3ζ results in proportional GFP expression in the A5-30FL-His reporter cells. Preincubation of Ba/F3-B7-H6 target cells with 30Stalk-His or 30LBD-His proteins blocks the effector-target cell interaction as indicated by the absence of GFP expression in the A5-30FL-His reporter cells. *E*, the Ba/F3-B7-H6 target cells were preincubated with blocking proteins (*red*, 30Stalk-His; *blue*, 30LBD-His; *dark gray*, 30Stalk-Ig; *light gray*, Ifnar2-Ig (control); concentrations are indicated) before co-incubation (16 h) with A5-30FL-His reporter cells. As control, A5-30FL-His reporter cells were preincubated with an anti-NKp30 antibody to inhibit signaling. For reference, corresponding signaling without blocking protein (*black*) was normalized to 100% GFP^+ A5-30FL-His reporter cells. *F*, binding of graded amounts of 30Stalk-His (*red square*, K_D 5 ± 3 nM), 30LBD-His (*blue circle*, K_D, 29 ± 1 nM), or MICA*04-His (*gray triangle*, control) proteins to recombinant B7-H6-Ig fusion protein by ELISA. Data were fit to a 1:1 Langmuir binding model to determine equilibrium binding constants (K_D). A representative of eight independent experiments is shown. *G*, binding of 30Stalk-His (*red*, 100 nM) or 30LBD-His proteins (*blue*, 100 nM) to recombinant B7-H6-Ig fusion proteins analyzed by ELISA. Preincubation of the 30Stalk-His proteins with an anti-NKp30 antibody (*white*) specifically blocks the NKp30-B7-H6 interaction. Notably, analogous blocking was observed for the 30LBD-His proteins (not shown). A representative of five independent experiments is shown. *H*, K_D values of different NKp30 ectodomain proteins.

top). These data imply that the number of clusters is mainly dependent on the ligand concentration on the target cell. By contrast, the mean cluster size after binding of 30Stalk-His proteins was significantly increased when compared with the clusters induced by 30LBD-His proteins. Therefore, we hypothesize that the stalk domain of NKp30 promotes formation of oligomeric receptor-ligand complexes (Fig. 3*C*, *bottom*).

To test whether the soluble ectodomain variants of NKp30 can inhibit a productive NKp30-dependent NK cell/target cell interaction, we performed signaling reporter assays in the absence and presence of 30Stalk-His and 30LBD-His proteins. Therefore, we used the A5-30FL-His reporter cell line as an effector cell that couples NKp30/CD3ζ chain-dependent signaling to correlated GFP expression (Fig. 3*D*) (34). Ba/F3-

B7-H6 cells were used as target cells. The percentage of GFP expressing A5-30FL-His reporter cells was quantified by flow cytometry (Fig. 3*E*). In the absence of NKp30 ectodomain proteins, Ba/F3-B7-H6 cells induced robust NKp30-dependent signaling of the A5-30FL-His reporter cells, which could be inhibited by an anti-NKp30 blocking antibody or NKp30::IgG1-Fc proteins but was not influenced by a non-relevant control protein (Ifnar2-Ig). Strikingly, both the 30Stalk-His and 30LBD-His proteins were efficient competitors of NKp30-dependent signaling, indicating their ligand specificity. Importantly, quantitative blocking of the NKp30/B7-H6 interaction was achieved already at a concentration of 3.1 μM for the 30Stalk-His protein, whereas inhibition remained incomplete (75%) for the 30LBD-His proteins even at a 7-fold higher concentration of 21.6 μM (Fig. 3*E*). In conclusion, these studies show that the ectodomain of NKp30 produced in insect cells specifically recognizes its ligand B7-H6 on target cells with a strong contribution of its stalk domain to high affinity binding.

To determine the apparent ligand binding affinities of the soluble 30Stalk-His and 30LBD-His proteins, we performed ELISA assays with recombinant B7-H6-Ig fusion protein. Therefore, B7-H6-Ig was immobilized and probed with graded amounts of 30Stalk-His and 30LBD-His proteins before detection of ligand-bound NKp30 with a polyclonal anti-NKp30 antibody. Both NKp30 variants bound specifically and dose-dependently to B7-H6-Ig with very low equilibrium binding constants (K_D values) of 5 $\pm$ 3 nM and 29 $\pm$ 1 nM for the 30Stalk-His and the 30LBD-His proteins, respectively (Fig. 3, *F*, *G*, and *H*). Surprisingly, these apparent binding affinities are higher than those published for the monovalent NKp30 ectodomain proteins refolded from *E. coli* inclusion bodies (1000 $\pm$ 200 nM (36) and the bivalent 30Stalk-Ig (76 $\pm$ 20 nM) and 30LBD-Ig (149 $\pm$ 19 nM) fusion proteins (34) (Fig. 3*H*). Therefore, these data suggest that NKp30 might form higher molecular order complexes that display a higher apparent ligand binding affinity by increased avidity of the oligomeric complex. Notably, the B_{max} values, an indicator for the maximum number of ligand binding receptive receptors in the solution, of the 30Stalk-His and the 30LBD-His proteins for binding to B7-H6-Ig were drastically different (Fig. 3*F*). This observation argues for a stalk-dependent difference in the architecture of the oligomeric self-assembly of the 30Stalk-His and the 30LBD-His proteins, which might in turn lead to a different degree of avidity and apparent affinity to B7-H6-Ig. This hypothesis is also supported by the much stronger inhibition of NKp30/B7-H6-dependent signaling of A5-30FL-His reporter cells by the 30Stalk-His proteins when compared with the bivalent 30Stalk-Ig proteins (Fig. 3*E*).

The Ectodomain of NKp30 Self-assembles Oligomers—To investigate oligomerization of NKp30, we performed size exclusion chromatography using a Superdex 200 column. Surprisingly, we found equilibria of three major species of proteins in solutions of 30Stalk-His and 30LBD-His proteins corresponding to monomers, dimers, and oligomers of soluble NKp30 (Fig. 4, *A* and *B*). Interestingly, the relative content of oligomers was much higher for the 30Stalk-His when compared with the 30LBD-His proteins. Notably, the degree of oligomerization and the relative ratio of oligomers, dimers, and monomers was dependent on the concentration of the protein solution, with a tendency to oligomer formation at higher protein concentrations. However, even at higher protein concentrations, the molar mass of the oligomers remained constant demonstrating formation of oligomers rather than non-functional aggregates. Notably, after isolation and concentration of individual peaks, the distribution of NKp30 species was restored (data not shown). With reference to size exclusion chromatography runs with a commercial calibration standard, the molecular mass of the oligomers was estimated at 250–290 kDa (elution volume 12 ml, corresponding to 14–16 30LBD-His monomers) and 360–440 kDa (elution volume 9.5 ml, corresponding to 18–22 30Stalk-His monomers). Because of the intrinsic capacity of 30LBD-His and the drastically increased tendency of the 30Stalk-His proteins to oligomerize, we propose two specific binding sites that contribute to NKp30 self-assembly.

Oligomerization of the NKp30 Ectodomain Increases Its Ligand Binding Affinity—Although our results suggest an avidity-driven increase of the apparent affinity of the 30Stalk-His and 30LBD-His proteins (Fig. 3*F*), so far the functional significance of the NKp30 ectodomain oligomers was uncertain. Therefore, we probed fractions from size exclusion chromatography that contained 30Stalk-His or 30LBD-His proteins, as determined by ELISA (Fig. 4, *C* and *D*), for binding to B7-H6-Ig in an ELISA setup described above. Strikingly, all of the oligomeric species (monomers, dimers, and oligomers) of soluble NKp30 bound to B7-H6-Ig (Fig. 4, *E* and *F*). In accordance with previous data, binding of 30Stalk-His proteins to B7-H6-Ig was stronger than that of 30LBD-His proteins, demonstrating again the importance of the stalk domain for ligand binding. Moreover, ELISA binding assays with separated 30Stalk-His oligomers, dimers, and monomers probed with recombinant B7-H6-Ig showed that the NKp30 oligomers have a higher affinity for B7-H6 than the dimeric or monomeric NKp30 as indicated by their trend to lower K_D and B_{max} values (Table 1). However, the observed differences are small and thus are difficult to interpret.

The Stalk Domain Contributes to Formation of NKp30 Oligomers—To study the geometry of the oligomers formed by 30Stalk-His and 30LBD-His proteins, we isolated the oligomers of both proteins by size exclusion chromatography. The oligomers were purified on a Superose 6 column for improved separation of large protein complexes. Although the individual peaks of the monomers and dimers could not be resolved on this column, we again observed monodisperse peaks of the expected molecular mass for the NKp30 ectodomain oligomers (Fig. 5, *A* and *C*). The elution fractions corresponding to the peak maxima of the oligomers of the 30Stalk-His or 30LBD-His proteins were analyzed by electron microscopy. After immobilization of the proteins on an EM grid, complexes were stained with uranyl acetate and subjected to electron microscopy. Strikingly, we observed particles with a diameter of about 15 nm for both NKp30 ectodomain constructs, demonstrating formation of oligomers rather than non-functional aggregates. Interestingly, the 30LBD-His oligomers appeared more homogeneous than the 30Stalk-His oligomers (Fig. 5, *B* and *D*). These data demonstrate that the ectodomain of NKp30 has an intrinsic ability to form oligomers with a contribution of the stalk

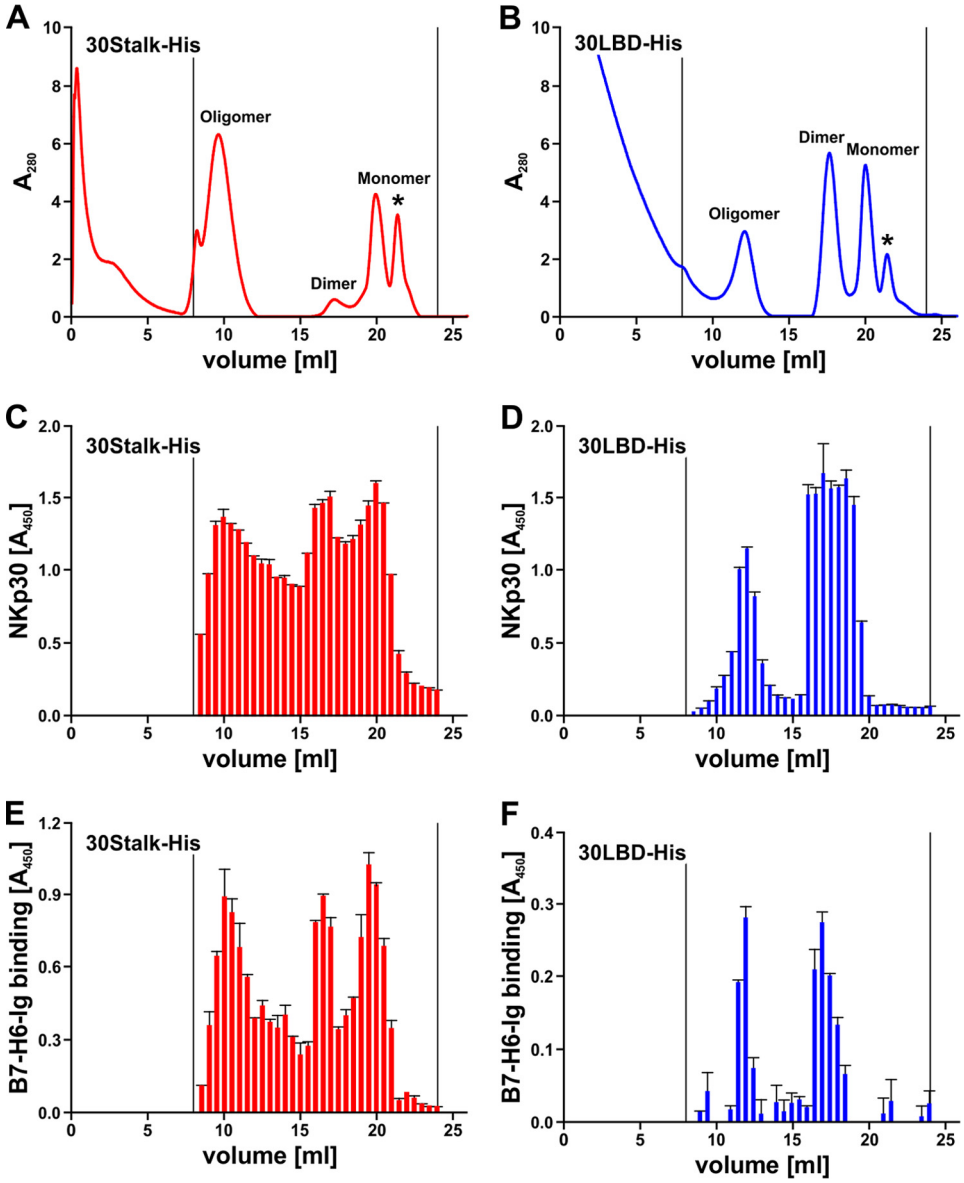

FIGURE 4. **The ectodomain of NKp30 self-assembles oligomers, which bind to its ligand B7-H6.** *A* and *B*, oligomers, dimers, and monomers of 30Stalk-His (*A*) and 30LBD-His (*B*) proteins were separated by size exclusion chromatography (Superdex 200 10/300 GL column). *Asterisk*, lower molecular weight compounds. *C* and *D*, elution fractions (500 μl) of size exclusion chromatography containing 30Stalk-His (*C*) and 30LBD-His (*D*) proteins were identified by ELISA with an anti-NKp30 antibody. *E* and *F*, specific binding of different oligomeric species of 30Stalk-His (*E*) and 30LBD-His (*F*) proteins to recombinant B7-H6-Ig fusion protein was validated by ELISA using an anti-NKp30 antibody.

TABLE 1

K_D and B_{max} values of B7-H6-Ig binding by different oligomeric species of 30Stalk-His proteins

30Stalk-His	K_D	B_{max}
	nM	
Mixture	0.92 ± 0.22	0.99 ± 0.03
Oligomers	1.04 ± 0.21	1.12 ± 0.03
Dimers	1.36 ± 0.10	0.84 ± 0.01
Monomers	1.90 ± 0.09	0.68 ± 0.01

domain to alignment of NKp30 within the oligomer. NKp30 oligomerization in turn leads to an increase in apparent ligand binding affinity by increased binding avidity. This might be of particular importance considering that IL-2 leads to a drastic up-regulation of NCR expression on the plasma membrane of NK cells, which will in turn promote the formation of NKp30 oligomers. Therefore, we propose self-association of NKp30 as a part of a mechanism to enhance ligand binding capacities and signaling within the immunological synapse.

DISCUSSION

NK cell cytotoxicity depends on the natural cytotoxicity receptors, as reduced NCR expression is associated with different forms of cancer such as acute myeloid leukemia (49–52). Tumor immunosurveillance by NK cells depends on the activating NK cell receptor NKp30. Notably, it is still unknown how this germ line-encoded NCR is able to recognize multiple ligands like viral hemagglutinins or proteins from bacterial or parasitical origin that are not related in sequence or structure (53–55). Moreover, because there is no orthologue in mice, it is tempting to speculate that NKp30 has evolved to additionally recognize up-regulated cellular ligands on transformed cells

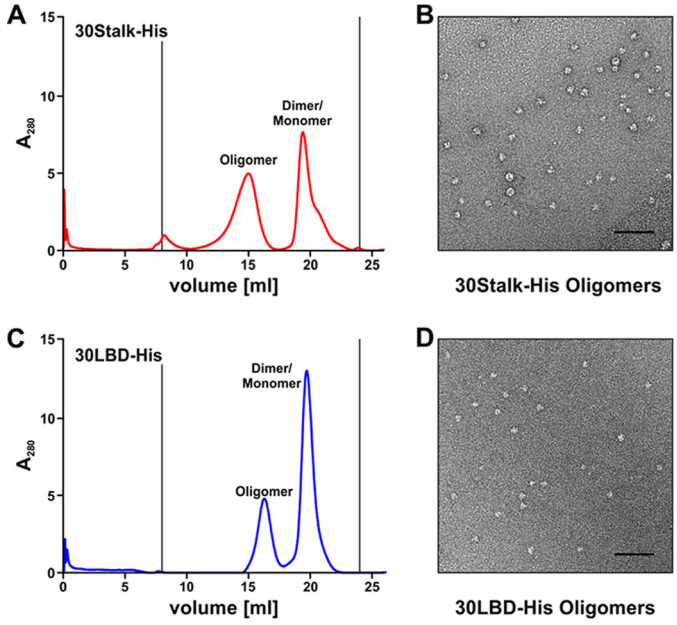

FIGURE 5. **The stalk domain modulates the geometry of the NKp30 ectodomain oligomers.** *A* and *C*, 30Stalk-His (*A*) and 30LBD-His (*C*) oligomers were separated from the monomer/dimer fractions by size exclusion chromatography (Superose 6 10/300 GL column). 100 μl elution fractions were collected. *B* and *D*, geometry and three-dimensional arrangement of the 30Stalk-His (*B*) and 30LBD-His (*D*) oligomers were analyzed by electron microscopy using the oligomer elution fractions with the highest protein amount from size exclusion chromatography (see *A* and *C*). *Bars* correspond to 100 nm.

like BAG-6 or B7-H6 (28, 29). Therefore, the molecular understanding of the NKp30 function in tumor immunosurveillance is instrumental in discovering novel access points for the development of new tumor therapies.

Within the current study, we have used insect cells to express functional NKp30 ectodomain proteins (30Stalk-His and 30LBD-His). These NKp30 variants were *N*-linked-glycosylated at three previously discovered acceptor sites (Asn-42, -68, and -121) and displayed a beneficial effect of the stalk domain on ligand binding (34). Surprisingly, these NKp30 ectodomain proteins exhibited a considerably higher affinity to the recombinant ligand B7-H6-Ig than the bivalent NKp30-Ig fusion proteins (34) or the *E. coli*-derived NKp30 ectodomain employed to determine the structure of the NKp30-B7-H6 complex (36). This increased affinity is due to an avidity effect, which is attributed to NKp30 ectodomain oligomerization. Notably, previous studies with *E. coli*-derived ectodomains of NKp30 demonstrated monovalency of the proteins in size exclusion chromatography (35, 36). By contrast, we found an equilibrium of monomers, dimers, and oligomers for both the glycosylated 30Stalk-His and 30LBD-His proteins derived from insect cells. EM analyses of isolated oligomer fractions of 30Stalk-His and 30LBD-His revealed differences in three-dimensional arrangement and geometry dependent on the stalk domain. Based on these data, we suggest two distinct sites for NKp30 ectodomain homo-oligomerization, one present within the Ig domain of NKp30 and one within its membrane proximal stalk domain. Similarly, the natural killer cell receptor KIR2DL2 dimerizes with both receptor ectodomain molecules in the same orientation via two different interaction sites. Therefore, Snyder and co-workers (56) suggested formation of KIR2DL2 oligomers within the plasma membrane by alternating dimerization. By contrast, the activating NK cell receptor NKG2D assembles a composite binding site for the interaction with its corresponding cellular ligands by homo-dimerization (57, 58).

The natural cytotoxicity receptors NKp46, NKp44, and NKp30 are type I transmembrane proteins that belong to the Ig superfamily. All of the NCRs consist of a crystallizable extracellular Ig domain, which is connected via a proximal stalk domain to the transmembrane domain followed by a short cytoplasmic tail (35–37, 59). However, it appears that the NCRs are much more different than anticipated from their domain organization and structure.

NKp30 is known to be only *N*-linked-glycosylated, which is important for ligand binding (34), whereas the *O*-glycosylation of NKp46 at position 225 is essential for binding to viral hemagglutinins (60). Along this line, there are also variations in the contribution of the NCR stalk domains on ligand binding and signaling. Sialic acid moieties attached to the stalk domain of NKp44 bind to viral hemagglutinin proteins (53, 61, 62), whereas the stalk domain of NKp30 displays a completely different mode of action as demonstrated in the current study and in a previous publication of our group (34). As suggested from the structures, monovalent receptor ligand interactions are expected for the NCRs. Strikingly, our current study shows that NKp30 oligomerization leads to formation of ligand binding competent multivalent complexes. Formation of *de novo* binding places by homo-oligomerization of the NKp30 ectodomains could be an additional mechanism of how the NK cell is able to recognize multiple different ligands. This observation has not been described for the other NCRs. Notably, NKp46 is able to form ligand binding-induced dimers most likely via its membrane proximal domain NKp46D2, which in turn leads to intracellular signaling (38). However, the precise dimerization interface of NKp46 remains unclear as steric hindrance and a possible direct contribution of the epitope sequence of the antibody to dimerization could not be distinguished in these studies.

Interestingly, oligomerization of proteins is a common principle in nature as illustrated by the fact that >35% of all proteins within a cell are oligomers (63–65). Therefore, oligomerization of NKp30 is likely to be of physiological relevance. In this context, it is known that IL-2 activation of NK cells leads to an up-regulation of NCR expression and thereby increases cellular cytotoxicity (22–27). This is in line with our observations from size exclusion chromatography demonstrating a concentration-dependent equilibrium of monomers, dimers, and oligomers for both 30Stalk-His and 30LBD-His. From a biochemical perspective, an increased concentration of NKp30 within the plasma membrane of an NK cell will shift the equilibrium toward oligomerization of the receptor. An appealing consideration for this hypothesis is that receptor oligomerization before ligand interaction would lead to faster activation of signaling. Notably, local concentration and oligomerization might even be fostered by ligand-induced assembly of a condensed immunological synapse between the NK cell and its target cell.

The precise orientation of the NKp30 ectodomains within the oligomers remains unknown. For the NK cell-target cell interaction a head-to-head orientation is most plausible. How-

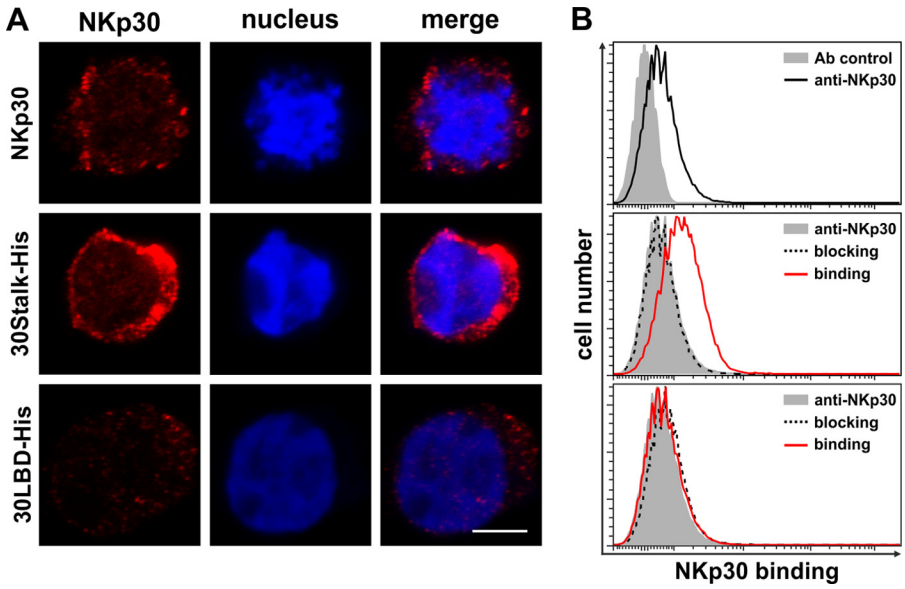

FIGURE 6. **The stalk domain of NKp30 is essential for recognition of NKp30 on NK cells *in trans*.** *A*, NK-92MI cells were decorated with anti-NKp30 antibodies, 30Stalk-His, or 30LBD-His proteins. Binding of the NKp30 ectodomain proteins was detected with an anti-NKp30 antibody. The degree of surface staining was monitored by CLSM (*red*, anti-NKp30; *blue*, DAPI; the *bar* corresponds to 4 μm). *B*, quantification of surface decoration of primary NK cells by flow cytometry. Cells were stained with an anti-NKp30 antibody (*black line*) to quantify the level of NKp30 surface expression (*solid gray*, antibody control). Binding of 30Stalk-His and 30LBD-His proteins (*red lines*) on primary NK cells and specific blocking with an anti-NKp30 blocking antibody (*dashed lines*) were analyzed (*solid gray*, NKp30 surface expression).

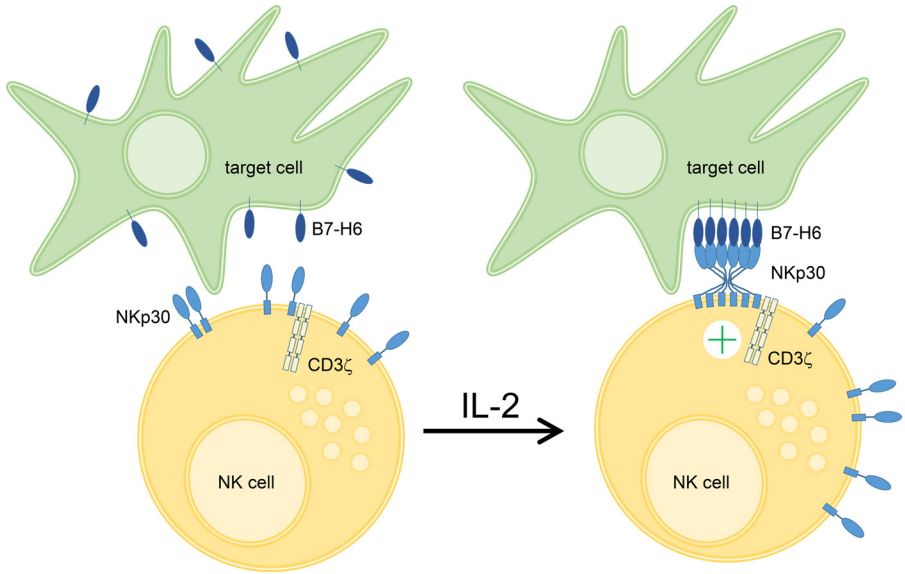

FIGURE 7. **NKp30 oligomerization drives NK cell cytotoxicity.** Upon IL-2 stimulation a variety of activating NK cell receptors including NKp30 are up-regulated on the plasma membrane of NK cells. Based on our data, we hypothesize that increased plasma membrane NKp30 leads to formation of NKp30 oligomers, which contact cellular ligands in the plasma membrane of target cells. This interaction is mediated by two binding sites within the NKp30 ectodomain resulting in increased ligand binding affinity or even *de novo* formation of composite binding sites. Finally, these presumably cooperative receptor-ligand interactions promote robust NKp30-dependent NK cell cytotoxicity.

ever, based on decoration experiments with 30Stalk-His protein and primary NK cells (Fig. 6), a head-to-tail orientation remains an additional possibility. Notably, this type of interaction is strictly dependent on the stalk domain of NKp30 as no decoration of primary NK cells was observed with 30LBD-His proteins. These findings are in accordance with the identification of a head-to-tail dimer in the crystal structure of the NKp30 ectodomain derived from *E. coli* (35). However, it remains obscure whether this head-to-tail dimer is of physiological relevance or a product of crystallization. Beside NK cells, NKp30 is expressed by distinct T cell subsets (66–69). Therefore, a head-to-tail interaction of NKp30 could provide a way for NK cells to bind to other immune cells expressing surface NKp30. This could be important for the regulation of immune responses.

In conclusion, we could show for the first time that the ectodomain of NKp30 self-assembles oligomers to increase its ligand binding affinity. Oligomerization involves two interaction sites, which are localized in the Ig domain and stalk domain of NKp30. Based on these data, we suggest that oligomerization

of the NKp30 ectodomain is a mechanism to modulate the ligand binding affinity of NKp30 by increased avidity and might even lead to *de novo* formation of a composite binding site for corresponding ligands. Because the degree of oligomerization is dependent on the local receptor concentration, which is up-regulated by IL-2 upon NK cell activation, oligomerization of NKp30 might be a molecular transformer of NK cell activation into enhanced cytotoxicity (Fig. 7).

Acknowledgments—We thank Dr. Roy Mariuzza (University of Maryland, Rockville, MD) for critical reading of the manuscript and helpful discussions. Moreover, we kindly acknowledge Dr. Carsten Watzl (IfADo), Dr. Andreas Diefenbach (University of Freiburg, Germany), Dr. Alexander Steinle (Goethe-University, Frankfurt am Main, Germany), and Dr. Imre Berger (EMBL, Grenoble, France) for providing cells, reagents, and related technical advice. The Georg-Speyer-Haus is supported jointly by the German Federal Ministry of Health (BMG) and the Ministry of Higher Education, Research, and the Arts of the State of Hessen (HMWK).

REFERENCES

1. Vivier, E., Ugolini, S., Blaise, D., Chabannon, C., and Brossay, L. (2012) Targeting natural killer cells and natural killer T cells in cancer. *Nat. Rev. Immunol.* **12,** 239–252
2. Groth, A., Klöss, S., von Strandmann, E. P., Koehl, U., and Koch, J. (2011) Mechanisms of tumor and viral immune escape from natural killer cell-mediated surveillance. *J. Innate Immun.* **3,** 344–354
3. Funke, J., Dürr, R., Dietrich, U., and Koch, J. (2011) Natural killer cells in HIV-1 infection. A double-edged sword. *AIDS Rev.* **13,** 67–76
4. Koch, J., Steinle, A., Watzl, C., and Mandelboim, O. (2013) Activating natural cytotoxicity receptors of natural killer cells in cancer and infection. *Trends Immunol.* **34,** 182–191
5. Moretta, L., Bottino, C., Pende, D., Castriconi, R., Mingari, M. C., and Moretta, A. (2006) Surface NK receptors and their ligands on tumor cells. *Semin. Immunol.* **18,** 151–158
6. Lanier, L. L. (1998) NK cell receptors. *Annu. Rev. Immunol.* **16,** 359–393
7. Moretta, A., Marcenaro, E., Parolini, S., Ferlazzo, G., and Moretta, L. (2008) NK cells at the interface between innate and adaptive immunity. *Cell death Differ.* **15,** 226–233
8. Wehner, R., Dietze, K., Bachmann, M., and Schmitz, M. (2011) The bidirectional crosstalk between human dendritic cells and natural killer cells. *J. Innate Immun.* **3,** 258–263
9. Vivier, E., Raulet, D. H., Moretta, A., Caligiuri, M. A., Zitvogel, L., Lanier, L. L., Yokoyama, W. M., and Ugolini, S. (2011) Innate or adaptive immunity? The example of natural killer cells. *Science* **331,** 44–49
10. Farag, S. S., and Caligiuri, M. A. (2006) Human natural killer cell development and biology. *Blood Rev.* **20,** 123–137
11. Kaifu, T., Escalière, B., Gastinel, L. N., Vivier, E., and Baratin, M. (2011) B7-H6/NKp30 interaction. A mechanism of alerting NK cells against tumors. *Cell. Mol. Life Sci.* **68,** 3531–3539
12. Lanier, L. L. (2005) NK cell recognition. *Annu. Rev. Immunol.* **23,** 225–274
13. Lisnić, V. J., Krmpotić, A., and Jonjić, S. (2010) Modulation of natural killer cell activity by viruses. *Curr. Opin. Microbiol.* **13,** 530–539
14. Lodoen, M. B., and Lanier, L. L. (2005) Viral modulation of NK cell immunity. *Nat. Rev. Microbiol.* **3,** 59–69
15. Seidel, E., Glasner, A., and Mandelboim, O. (2012) Virus-mediated inhibition of natural cytotoxicity receptor recognition. *Cell. Mol. Life Sci.* **69,** 3911–3920
16. Watzl, C., and Long, E. O. (2010) Signal transduction during activation and inhibition of natural killer cells. *Curr. Protoc. Immunol.* Chapter 11, Unit 11.9B
17. Sivori, S., Vitale, M., Morelli, L., Sanseverino, L., Augugliaro, R., Bottino, C., Moretta, L., and Moretta, A. (1997) p46, a novel natural killer cell-specific surface molecule that mediates cell activation. *J. Exp. Med.* **186,** 1129–1136
18. Pessino, A., Sivori, S., Bottino, C., Malaspina, A., Morelli, L., Moretta, L., Biassoni, R., and Moretta, A. (1998) Molecular cloning of NKp46. A novel member of the immunoglobulin superfamily involved in triggering of natural cytotoxicity. *J. Exp. Med.* **188,** 953–960
19. Vitale, M., Bottino, C., Sivori, S., Sanseverino, L., Castriconi, R., Marcenaro, E., Augugliaro, R., Moretta, L., and Moretta, A. (1998) NKp44, a novel triggering surface molecule specifically expressed by activated natural killer cells, is involved in non-major histocompatibility complex-restricted tumor cell lysis. *J. Exp. Med.* **187,** 2065–2072
20. Cantoni, C., Bottino, C., Vitale, M., Pessino, A., Augugliaro, R., Malaspina, A., Parolini, S., Moretta, L., Moretta, A., and Biassoni, R. (1999) NKp44, a triggering receptor involved in tumor cell lysis by activated human natural killer cells, is a novel member of the immunoglobulin superfamily. *J. Exp. Med.* **189,** 787–796
21. Pende, D., Parolini, S., Pessino, A., Sivori, S., Augugliaro, R., Morelli, L., Marcenaro, E., Accame, L., Malaspina, A., Biassoni, R., Bottino, C., Moretta, L., and Moretta, A. (1999) Identification and molecular characterization of NKp30, a novel triggering receptor involved in natural cytotoxicity mediated by human natural killer cells. *J. Exp. Med.* **190,** 1505–1516
22. Kloess, S., Huenecke, S., Piechulek, D., Esser, R., Koch, J., Brehm, C., Soerensen, J., Gardlowski, T., Brinkmann, A., Bader, P., Passweg, J., Klingebiel, T., Schwabe, D., and Koehl, U. (2010) IL-2-activated haploidentical NK cells restore NKG2D-mediated NK-cell cytotoxicity in neuroblastoma patients by scavenging of plasma MICA. *Eur. J. Immunol.* **40,** 3255–3267
23. Kajitani, K., Tanaka, Y., Arihiro, K., Kataoka, T., and Ohdan, H. (2012) Mechanistic analysis of the antitumor efficacy of human natural killer cells against breast cancer cells. *Breast Cancer Res. Treat* **134,** 139–155
24. Ferlazzo, G., Thomas, D., Lin, S. L., Goodman, K., Morandi, B., Muller, W. A., Moretta, A., and Münz, C. (2004) The abundant NK cells in human secondary lymphoid tissues require activation to express killer cell Ig-like receptors and become cytolytic. *J. Immunol.* **172,** 1455–1462
25. Mavilio, D., Benjamin, J., Daucher, M., Lombardo, G., Kottilil, S., Planta, M. A., Marcenaro, E., Bottino, C., Moretta, L., Moretta, A., and Fauci, A. S. (2003) Natural killer cells in HIV-1 infection. Dichotomous effects of viremia on inhibitory and activating receptors and their functional correlates. *Proc. Natl. Acad. Sci. U.S.A.* **100,** 15011–15016
26. Moretta, A., Bottino, C., Vitale, M., Pende, D., Cantoni, C., Mingari, M. C., Biassoni, R., and Moretta, L. (2001) Activating receptors and coreceptors involved in human natural killer cell-mediated cytolysis. *Annu. Rev. Immunol.* **19,** 197–223
27. Rosenberg, S. A., and Lotze, M. T. (1986) Cancer immunotherapy using interleukin-2 and interleukin-2-activated lymphocytes. *Annu. Rev. Immunol.* **4,** 681–709
28. Brandt, C. S., Baratin, M., Yi, E. C., Kennedy, J., Gao, Z., Fox, B., Haldeman, B., Ostrander, C. D., Kaifu, T., Chabannon, C., Moretta, A., West, R., Xu, W., Vivier, E., and Levin, S. D. (2009) The B7 family member B7-H6 is a tumor cell ligand for the activating natural killer cell receptor NKp30 in humans. *J. Exp. Med.* **206,** 1495–1503
29. Pogge von Strandmann, E., Simhadri, V. R., von Tresckow, B., Sasse, S., Reiners, K. S., Hansen, H. P., Rothe, A., Böll, B., Simhadri, V. L., Borchmann, P., McKinnon, P. J., Hallek, M., and Engert, A. (2007) Human leukocyte antigen-B-associated transcript 3 is released from tumor cells and engages the NKp30 receptor on natural killer cells. *Immunity* **27,** 965–974
30. Simhadri, V. R., Reiners, K. S., Hansen, H. P., Topolar, D., Simhadri, V. L., Nohroudi, K., Kufer, T. A., Engert, A., and Pogge von Strandmann, E. (2008) Dendritic cells release HLA-B-associated transcript-3-positive exosomes to regulate natural killer function. *PLoS ONE* **3,** e3377
31. Reiners, K. S., Topolar, D., Henke, A., Simhadri, V. R., Kessler, J., Sauer, M., Bessler, M., Hansen, H. P., Tawadros, S., Herling, M., Krönke, M., Hallek, M., and Pogge von Strandmann, E. (2013) Soluble ligands for NK cell receptors promote evasion of chronic lymphocytic leukemia cells from NK cell anti-tumor activity. *Blood* **121,** 3658–3665
32. Binici, J., Hartmann, J., Herrmann, J., Schreiber, C., Beyer, S., Guler, G., Vogel, V., Tumulka, F., Abele, R., Mantele, W., and Koch, J. (2013) A soluble fragment of the tumor antigen BCL2-associated athanogene 6 (BAG-6) is essential and sufficient for inhibition of NKp30-dependent cytotoxicity of natural killer cells. *J. Biol. Chem.* **288,** 34295–34303

33. Binici, J., and Koch, J. (2013) BAG-6, a jack of all trades in health and disease. *Cell. Mol. Life Sci.* 10.1007/s00018-013-1522-y
34. Hartmann, J., Tran, T. V., Kaudeer, J., Oberle, K., Herrmann, J., Quagliano, I., Abel, T., Cohnen, A., Gatterdam, V., Jacobs, A., Wollscheid, B., Tampé, R., Watzl, C., Diefenbach, A., and Koch, J. (2012) The stalk domain and the glycosylation status of the activating natural killer cell receptor NKp30 are important for ligand binding. *J. Biol. Chem.* **287,** 31527–31539
35. Joyce, M. G., Tran, P., Zhuravleva, M. A., Jaw, J., Colonna, M., and Sun, P. D. (2011) Crystal structure of human natural cytotoxicity receptor NKp30 and identification of its ligand binding site. *Proc. Natl. Acad. Sci. U.S.A.* **108,** 6223–6228
36. Li, Y., Wang, Q., and Mariuzza, R. A. (2011) Structure of the human activating natural cytotoxicity receptor NKp30 bound to its tumor cell ligand B7-H6. *J. Exp. Med.* **208,** 703–714
37. Cantoni, C., Ponassi, M., Biassoni, R., Conte, R., Spallarossa, A., Moretta, A., Moretta, L., Bolognesi, M., and Bordo, D. (2003) The three-dimensional structure of the human NK cell receptor NKp44, a triggering partner in natural cytotoxicity. *Structure* **11,** 725–734
38. Jaron-Mendelson, M., Yossef, R., Appel, M. Y., Zilka, A., Hadad, U., Afergan, F., Rosental, B., Engel, S., Nedvetzki, S., Braiman, A., and Porgador, A. (2012) Dimerization of NKp46 receptor is essential for NKp46-mediated lysis. Characterization of the dimerization site by epitope mapping. *J. Immunol.* **188,** 6165–6174
39. Vivier, E., Tomasello, E., Baratin, M., Walzer, T., and Ugolini, S. (2008) Functions of natural killer cells. *Nat. Immunol.* **9,** 503–510
40. Brown, A. C., Oddos, S., Dobbie, I. M., Alakoskela, J. M., Parton, R. M., Eissmann, P., Neil, M. A., Dunsby, C., French, P. M., Davis, I., and Davis, D. M. (2011) Remodelling of cortical actin where lytic granules dock at natural killer cell immune synapses revealed by super-resolution microscopy. *PLoS Biol.* **9,** e1001152
41. Rak, G. D., Mace, E. M., Banerjee, P. P., Svitkina, T., and Orange, J. S. (2011) Natural killer cell lytic granule secretion occurs through a pervasive actin network at the immune synapse. *PLoS Biol.* **9,** e1001151
42. Grave, L., Tůmová, L., Mrázek, H., Kavan, D., Chmelík, J., Vaněk, O., Novák, P., and Bezouška, K. (2012) Preparation of soluble isotopically labeled NKp30, a human natural cytotoxicity receptor, for structural studies using NMR. *Protein Expr. Purif.* **86,** 142–150
43. Jarahian, M., Fiedler, M., Cohnen, A., Djandji, D., Hämmerling, G. J., Gati, C., Cerwenka, A., Turner, P. C., Moyer, R. W., Watzl, C., Hengel, H., and Momburg, F. (2011) Modulation of NKp30- and NKp46-mediated natural killer cell responses by poxviral hemagglutinin. *PLoS Pathog.* **7,** e1002195
44. Andersen, P. S., Menné, C., Mariuzza, R. A., Geisler, C., and Karjalainen, K. (2001) A response calculus for immobilized T cell receptor ligands. *J. Biol. Chem.* **276,** 49125–49132
45. Trowitzsch, S., Bieniossek, C., Nie, Y., Garzoni, F., and Berger, I. (2010) New baculovirus expression tools for recombinant protein complex production. *J. Struct. Biol.* **172,** 45–54
46. Lamken, P., Gavutis, M., Peters, I., Van der Heyden, J., Uzé, G., and Piehler, J. (2005) Functional cartography of the ectodomain of the type I interferon receptor subunit ifnar1. *J. Mol. Biol.* **350,** 476–488
47. Li, P., Morris, D. L., Willcox, B. E., Steinle, A., Spies, T., and Strong, R. K. (2001) Complex structure of the activating immunoreceptor NKG2D and its MHC class I-like ligand MICA. *Nat. Immunol.* **2,** 443–451
48. Carpenter, A. E., Jones, T. R., Lamprecht, M. R., Clarke, C., Kang, I. H., Friman, O., Guertin, D. A., Chang, J. H., Lindquist, R. A., Moffat, J., Golland, P., and Sabatini, D. M. (2006) CellProfiler. Image analysis software for identifying and quantifying cell phenotypes. *Genome Biol.* **7,** R100
49. Fauriat, C., Just-Landi, S., Mallet, F., Arnoulet, C., Sainty, D., Olive, D., and Costello, R. T. (2007) Deficient expression of NCR in NK cells from acute myeloid leukemia. Evolution during leukemia treatment and impact of leukemia cells in NCRdull phenotype induction. *Blood* **109,** 323–330
50. Garcia-Iglesias, T., Del Toro-Arreola, A., Albarran-Somoza, B., Del Toro-Arreola, S., Sanchez-Hernandez, P. E., Ramirez-Dueñas, M. G., Balderas-Peña, L. M., Bravo-Cuellar, A., Ortiz-Lazareno, P. C., and Daneri-Navarro, A. (2009) Low NKp30, NKp46, and NKG2D expression and reduced cytotoxic activity on NK cells in cervical cancer and precursor lesions. *BMC Cancer* **9,** 186
51. Mamessier, E., Sylvain, A., Thibult, M. L., Houvenaeghel, G., Jacquemier, J., Castellano, R., Gonçalves, A., André, P., Romagné, F., Thibault, G., Viens, P., Birnbaum, D., Bertucci, F., Moretta, A., and Olive, D. (2011) Human breast cancer cells enhance self-tolerance by promoting evasion from NK cell antitumor immunity. *J. Clin. Invest.* **121,** 3609–3622
52. Pietra, G., Manzini, C., Rivara, S., Vitale, M., Cantoni, C., Petretto, A., Balsamo, M., Conte, R., Benelli, R., Minghelli, S., Solari, N., Gualco, M., Queirolo, P., Moretta, L., and Mingari, M. C. (2012) Melanoma cells inhibit natural killer cell function by modulating the expression of activating receptors and cytolytic activity. *Cancer Res.* **72,** 1407–1415
53. Mandelboim, O., Lieberman, N., Lev, M., Paul, L., Arnon, T. I., Bushkin, Y., Davis, D. M., Strominger, J. L., Yewdell, J. W., and Porgador, A. (2001) Recognition of haemagglutinins on virus-infected cells by NKp46 activates lysis by human NK cells. *Nature* **409,** 1055–1060
54. Mavoungou, E., Held, J., Mewono, L., and Kremsner, P. G. (2007) A Duffy binding-like domain is involved in the NKp30-mediated recognition of *Plasmodium falciparum*-parasitized erythrocytes by natural killer cells. *J. Infect Dis.* **195,** 1521–1531
55. Garg, A., Barnes, P. F., Porgador, A., Roy, S., Wu, S., Nanda, J. S., Griffith, D. E., Girard, W. M., Rawal, N., Shetty, S., and Vankayalapati, R. (2006) Vimentin expressed on *Mycobacterium tuberculosis*-infected human monocytes is involved in binding to the NKp46 receptor. *J. Immunol.* **177,** 6192–6198
56. Snyder, G. A., Brooks, A. G., and Sun, P. D. (1999) Crystal structure of the HLA-Cw3 allotype-specific killer cell inhibitory receptor KIR2DL2. *Proc. Natl. Acad. Sci. U.S.A.* **96,** 3864–3869
57. Garrity, D., Call, M. E., Feng, J., and Wucherpfennig, K. W. (2005) The activating NKG2D receptor assembles in the membrane with two signaling dimers into a hexameric structure. *Proc. Natl. Acad. Sci. U.S.A.* **102,** 7641–7646
58. Steinle, A., Li, P., Morris, D. L., Groh, V., Lanier, L. L., Strong, R. K., and Spies, T. (2001) Interactions of human NKG2D with its ligands MICA, MICB, and homologs of the mouse RAE-1 protein family. *Immunogenetics* **53,** 279–287
59. Foster, C. E., Colonna, M., and Sun, P. D. (2003) Crystal structure of the human natural killer (NK) cell activating receptor NKp46 reveals structural relationship to other leukocyte receptor complex immunoreceptors. *J. Biol. Chem.* **278,** 46081–46086
60. Arnon, T. I., Achdout, H., Lieberman, N., Gazit, R., Gonen-Gross, T., Katz, G., Bar-Ilan, A., Bloushtain, N., Lev, M., Joseph, A., Kedar, E., Porgador, A., and Mandelboim, O. (2004) The mechanisms controlling the recognition of tumor- and virus-infected cells by NKp46. *Blood* **103,** 664–672
61. Arnon, T. I., Lev, M., Katz, G., Chernobrov, Y., Porgador, A., and Mandelboim, O. (2001) Recognition of viral hemagglutinins by NKp44 but not by NKp30. *Eur. J. Immunol.* **31,** 2680–2689
62. Jarahian, M., Watzl, C., Fournier, P., Arnold, A., Djandji, D., Zahedi, S., Cerwenka, A., Paschen, A., Schirrmacher, V., and Momburg, F. (2009) Activation of natural killer cells by Newcastle disease virus hemagglutinin-neuraminidase. *J. Virol.* **83,** 8108–8121
63. Goodsell, D. S. (1991) Inside a living cell. *Trends Biochem. Sci.* **16,** 203–206
64. Goodsell, D. S., and Olson, A. J. (2000) Structural symmetry and protein function. *Annu. Rev. Biophys. Biomol. Struct.* **29,** 105–153
65. Ali, M. H., and Imperiali, B. (2005) Protein oligomerization. How and why. *Bioorg. Med. Chem.* **13,** 5013–5020
66. Tang, Q., Grzywacz, B., Wang, H., Kataria, N., Cao, Q., Wagner, J. E., Blazar, B. R., Miller, J. S., and Verneris, M. R. (2008) Umbilical cord blood T cells express multiple natural cytotoxicity receptors after IL-15 stimulation, but only NKp30 is functional. *J. Immunol.* **181,** 4507–4515
67. Correia, D. V., Fogli, M., Hudspeth, K., da Silva, M. G., Mavilio, D., and Silva-Santos, B. (2011) Differentiation of human peripheral blood Vd1+ T cells expressing the natural cytotoxicity receptor NKp30 for recognition of lymphoid leukemia cells. *Blood* **118,** 992–1001
68. Hudspeth, K., Fogli, M., Correia, D. V., Mikulak, J., Roberto, A., Della Bella, S., Silva-Santos, B., and Mavilio, D. (2012) Engagement of NKp30 on Vd1 T cells induces the production of CCL3, CCL4, and CCL5 and suppresses HIV-1 replication. *Blood* **119,** 4013–4016
69. Hudspeth, K., Silva-Santos, B., and Mavilio, D. (2013) Natural cytotoxicity receptors. Broader expression patterns and functions in innate and adaptive immune cells. *Front. Immunol.* **4,** 69